

# EarPass: Secure and Implicit Call Receiver Authentication Using Ear Acoustic Sensing

Xiping Sun, Jing Chen, Kun He, Zhixiang He, Ruiying Du, Yebo Feng, Qingchuan Zhao, Cong Wu

**Abstract**—Private voice communication often contains sensitive information, making it critical to ensure that only authorized users have access to such calls. Unfortunately, current authentication mechanisms, such as PIN-based passwords, fingerprint recognition, and face recognition, fail to authenticate the call receiver, leaving a gap in security. To fill the gap, we present EarPass, a secure and implicit call receiver authentication scheme designed for smartphones. EarPass sends inaudible acoustic signals through the earpiece speaker to actively sense the outer ear, and records echoes using the top microphone. It focuses on extracting ear-related signals from echoes and performs spectrogram analysis in the magnitude and phase domains. To overcome posture and position variability, EarPass utilizes a learning-based feature extractor for extracting representative features, and a one-class classifier for authentication. EarPass does not increase any burdens on users or change users’ call answering habits. Furthermore, it does not require extra devices but only uses the speaker and microphone on the smartphone. We conducted comprehensive experiments to evaluate EarPass’s effectiveness and security. Our results show that EarPass can achieve a balanced accuracy of 96.95% and an equal error rate of 1.53%. Additionally, EarPass exhibits resilience against potential attacks, including zero-effort attacks and mimicry attacks.

**Index Terms**—Call receiver authentication, acoustic sensing, behavior variability, smartphone.

## I. INTRODUCTION

SMARTPHONES have become an indispensable part of daily life. To prevent unauthorized access to smartphones, various user authentication mechanisms have been deployed, including PIN-based passwords, fingerprint recognition, and facial recognition. These methods provide users with a usable way to secure their devices and perform sensitive operations, such as online bank transactions. Unfortunately, there is cur-

Xiping Sun, Kun He, and Zhixiang He are with Key Laboratory of Aerospace Information Security and Trusted Computing, Ministry of Education, School of Cyber Science and Engineering, Wuhan University, Wuhan, China. Email: {xiping, hekun, zhixianghe}@whu.edu.cn.

Jing Chen is with Key Laboratory of Aerospace Information Security and Trusted Computing, Ministry of Education, School of Cyber Science and Engineering, Wuhan University, Wuhan, China, and also with Rizhao Institute of Information Technology, Wuhan University, Rizhao, China. Email: chenjing@whu.edu.cn.

Ruiying Du is with Key Laboratory of Aerospace Information Security and Trusted Computing, Ministry of Education, School of Cyber Science and Engineering, Wuhan University, Wuhan, China, and also with Collaborative Innovation Center of Geospatial Technology, Wuhan, China. Email: duraying@whu.edu.cn.

Yebo Feng and Cong Wu are with School of Computer Science and Engineering, Nanyang Technological University, Singapore. Email: {yebo.feng, cong.wu}@ntu.edu.sg.

Qingchuan Zhao is with Department of Computer Science, City University of Hong Kong. Email: cs.qczhao@cityu.edu.hk.

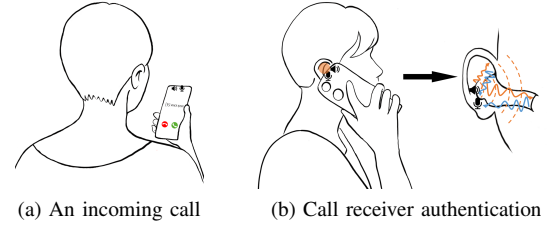


Fig. 1. Illustration of EarPass. When a call comes in, the user places the smartphone close to his/her ear to answer it. The earpiece speaker and top microphone serve as an active sonar to sense the user’s outer ear and then authenticate the identity of the call receiver.

rently no mechanism in place to determine if the person answering the call is the legitimate device owner.

For example, when users receive an incoming call on their smartphone, they are not required to perform any authentication to determine if they are the legitimate device owner. Even if the smartphone is locked, users can simply click the accept button to answer the call, whether it is a traditional phone call or a VoIP call through social apps like WhatsApp [1], WeChat [2] and DingTalk [3]. While voice communication content may be encrypted to prevent eavesdropping attacks [4] and caller authentication may block unwanted calls [5], the lack of user authentication on the call receiver side does not meet security requirements and can result in serious privacy disclosure. Therefore, it is crucial to design an appropriate authentication mechanism for the call receiver to ensure that only legitimate device owners can answer incoming calls.

Existing research has explored various approaches for providing call receiver authentication on smartphones, which can be classified into two main categories: behavioral characteristics of call answering [6]–[11], and physiological characteristics of the ear [12]–[18]. For example, [6]–[11] use motion sensors to capture the device’s movement and analyze the user’s arm motion behavior during call answering, aiming to distinguish between different users. Despite various attempts at call receiver authentication, existing methods have their limitations. For instance, arm motion-based methods may suffer from low accuracy due to behavioral variability [19]. Ear image-based methods rely on extra gestures and have limited authentication accuracy in low-light environments [12], [13]. Using the touchscreen as a capacitive sensor for ear authentication requires rooting the smartphone and modifying the kernel source [14], [15]. Additionally, acoustic sensing is explored to capture the physiological characteristics of the ear, but extra devices such as wireless earphones are necessary for these methods [16]–[18]. These limitations indicate the need

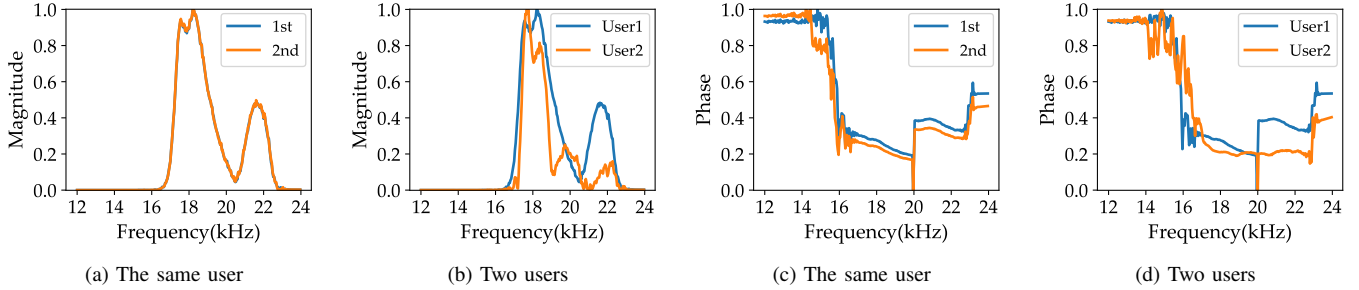


Fig. 2. The acoustic profiles of the ear-related signals for two users. (a) Magnitude spectrums for user 1 at two times. (b) Magnitude spectrums for two users. (c) Phase spectrums for user 1 at two times. (d) Phase spectrums for two users.

for an effective call receiver authentication mechanism that can provide a seamless user experience and is not dependent on external devices or smartphone modifications.

In this paper, we propose EarPass, a novel call receiver authentication scheme designed for smartphones. EarPass utilizes inaudible acoustic signals to extract features from the reflected signal by the outer ear, enabling secure and implicit authentication without any extra devices. The scheme is designed to authenticate the call receiver seamlessly without any additional burden on the user, ensuring a smooth and secure call answering experience. Unlike existing methods, EarPass can also enhance security by providing continuous authentication after one-time authentication. Additionally, EarPass is resilient against certain variations in human posture and smartphone position, making it more robust and easy to use.

Fig. 1 shows the process of call receiver authentication for EarPass. EarPass uses the earpiece speaker to send the inaudible signal for acoustic sensing and the top microphone to record echoes. After receiving the echoes, EarPass applies a bandpass filter to remove unwanted noise and performs signal segmentation to extract the target signal that is reflected by the outer ear. EarPass also selects a reference segment and extracts the absolute difference matrix of magnitude and phase spectrogram over different segments. Then, EarPass uses a CNN-based feature extractor to analyze the representative acoustic features. Finally, EarPass trains a one-class classification model to determine whether the call receiver is legitimate.

In summary, the contributions of this paper are as follows:

- We propose EarPass, a secure and implicit call receiver authentication scheme for smartphones. It works by transmitting inaudible sound to sense the outer ear, extracting acoustic features, and verifying the legitimacy of the call receiver. It is also available for continuous authentication.
- We design a signal synchronization and segmentation approach to accurately locate the ear-related reflected signal. We also devise a CNN-based feature extraction method that extracts effective and robust features from spectrograms to handle posture and position variability.
- We conduct comprehensive experiments under various conditions to evaluate the effectiveness of EarPass, e.g., ambient noises, different periods, different postures, and different devices. Our experimental results show that EarPass can achieve a balanced accuracy of 96.95% and a equal error rate of 1.53%, making it an effective and

practical authentication method.

- We demonstrate the security of EarPass by evaluating its effectiveness against common attacks. Our results indicate that EarPass is resistant to common attacks and offers a secure authentication solution for call receivers on smartphones.

## II. PRELIMINARIES

In this section, we introduce the unique structure of the ear and feasibility analysis for ear acoustic sensing.

### A. Structure of Ear

The human ear consists of three parts: the outer ear, the middle ear, and the inner ear. The outer ear, as the exterior part, interacts most directly with the external environment. It mainly contains two parts: the pinna and the ear canal. The pinna is a three-dimensional structure made up of cartilage and skin, which is distinctive to each individual [20]. The ear canal, a short tube terminating at the eardrum, displays variations in its interspace, curvature, and composition across populations [21]. Our goal is to utilize acoustic sensing to detect the distinctive outer ear characteristics of each individual for authentication.

### B. Ear Acoustic Sensing

To sense the outer ear using acoustic sensing, we use the earpiece speaker to emit inaudible sensing signals and the microphone to record echoes. Due to the multipath effect of sound propagation, the transmitted signals travel through different paths and arrive at the microphone with various delays. Specifically, the received signals comprise the direct path, ear reflections and other reflected signals. The direct path signals travel straight from the speaker to the microphone. The reflected signals experience absorption and reflection by obstacles, such as the ear and other objects. These received signals can reach the outer ear through different paths, resulting in changes in magnitude and phase. Our method focuses on extracting ear-related signals from the received signals and analyzing the characteristics of their magnitude and phase.

We present a toy example to explore the feasibility of distinguishing between different users based on the reflected signal from the outer ear. We employ two users to simulate the call answering process. The sensing signal utilized is a 25-millisecond chirp signal ranging from 17kHz to 23kHz. After

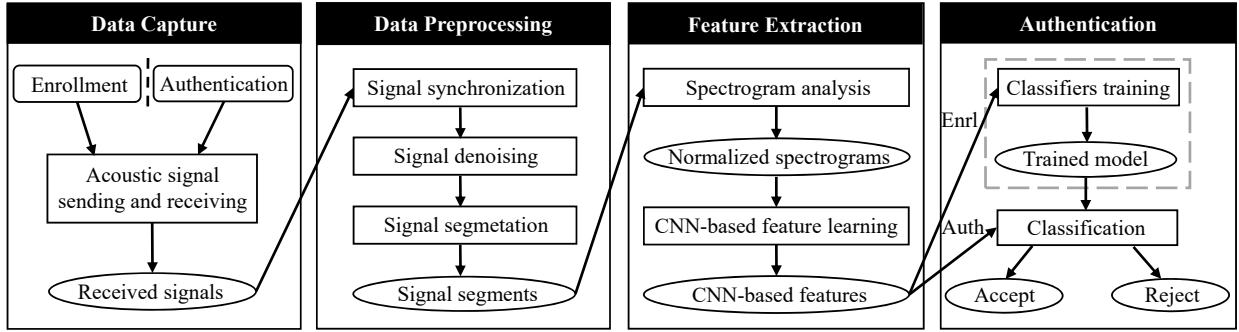


Fig. 3. Workflow of EarPass.

deriving the ear-related signals, we extract their magnitude and phase spectrums. Fig. 2 displays the results. Fig. 2(a) and Fig. 2(c) present magnitude and phase spectrums of two instances for user 1, respectively. Fig. 2(b) and Fig. 2(d) show magnitude and phase spectrums for two users (i.e., user 1 and user 2), respectively. We observe that the profiles of two instances for the same user match each other closely. In contrast, the profiles of the two users exhibit differences from each other. The results indicate the feasibility of ear acoustic sensing and motivate us to design EarPass.

### III. OVERVIEW OF EARPASS

In this section, we first present the overview of EarPass. Then we introduce the threat model and design goals.

#### A. System Overview

The basic idea of EarPass is to use the speaker and microphone on a smartphone for acoustic sensing, and then analyze ear-related features from the received acoustic signals to authenticate the call receiver. It consists of two phases: enrollment and authentication. In the enrollment phase, it leverages acoustic features to build the authentication model of the legitimate user. In the authentication phase, EarPass decides whether the call receiver is legitimate.

Fig. 3 shows the workflow of EarPass. It comprises four modules: data capture, data preprocessing, feature extraction, and authentication. The data capture module uses the smartphone's earpiece speaker and top microphone as an active sonar. It sends inaudible acoustic signals and records echoes. The data preprocessing module first performs signal synchronization between the smartphone speaker and microphone. Then it applies a bandpass filter to remove ambient noises and other interferences from the received signal, and performs signal segmentation to extract the target signal reflected by the outer ear. The feature extraction module first performs spectrogram analysis to obtain normalized spectrograms. Specifically, it applies Short-Time Fourier transform (STFT) to the extracted segments to get spectrograms, computes the absolute difference matrix between them, and performs min-max normalization. Then it extracts the representative acoustic features using a pre-trained convolution neural network model. The authentication module trains a one-class classification model during the enrollment phase based on the collected

samples from the legitimate user. After enrollment, the model determines whether the user is legitimate.

Instead of just one-time authentication, EarPass also supports continuous authentication by periodically sensing the outer ear. EarPass is an unobtrusive authentication approach with superb usability. It is inaudible to users and does not interfere with a normal voice conversation. Also, users are not required to perform any additional action and only need to keep listening to the smartphone.

#### B. Threat Model

For the sake of privacy, users generally choose earpiece mode instead of speaker mode to answer the call [22], which means users place the smartphone close to their ear and use the earpiece speaker to listen. Since voice communication content is encrypted from end to end [23], it is difficult for the attacker to eavesdrop on the call content over the audio channel. We assume that the attacker is near the victim's smartphone when the call comes, and the attacker's goal is to bypass EarPass to answer the call. There are two common attacks considering the attacker's ability and goal:

- *Zero-effort attack.* Without any prior knowledge of the legitimate user, the attacker tries to pass the call receiver authentication by chance.
- *Mimicry attack.* According to observing the authentication process of the legitimate user, the attacker attempts to pass the call receiver authentication by imitation.

#### C. Design Goals

We think a suitable authentication scheme for a call receiver should satisfy the following goals:

- *Accurate and secure:* it should accept the legitimate user at a high rate. Also, it should reject the unauthorized user accurately and defend against common attacks.
- *Implicit:* it should not change users' call answering habits and not interfere with a normal voice conversation. It should be easy to use for ordinary users and not require explicit user participation.
- *Universal:* it should not rely on extra devices to perform authentication. It works on common smartphones without requiring additional hardware or root privileges.
- *Robust:* it should perform robustly across various conditions, e.g., ambient noises, different periods, different postures, and different devices.

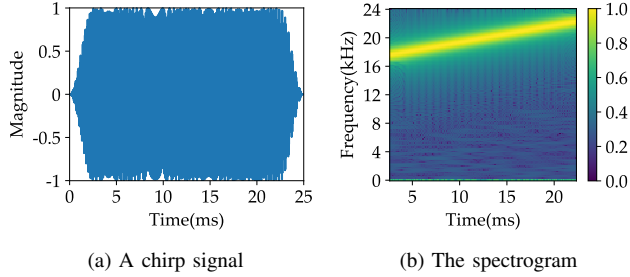


Fig. 4. An example of the sensing signal in time and frequency domains.

#### IV. DATA CAPTURE

In this section, we introduce the selection of the speaker and microphone, and illustrate the process of acoustic signal sending and receiving.

##### A. Speaker and Microphone Selection

Existing commodity smartphones are typically equipped with two speakers, including a main speaker positioned at the bottom and a top speaker (i.e., earpiece speaker) closer to the ear [24]. There are also a microphone at the bottom, and another at the top designed for noise cancellation [25], which is less likely to be affected by human factors such as hand posture compared with the bottom microphone. Therefore, we select the earpiece speaker and top microphone to send and receive signals, which are more suitable for robust ear acoustic sensing than other sensors.

##### B. Acoustic Signal Sending and Receiving

We choose the chirp signal as our sensing signal, whose frequency changes continuously with time. This signal possesses excellent auto-correlation characteristics and is widely used for acoustic sensing [26]. During sensing, the earpiece speaker plays the inaudible chirp signal, and the top microphone keeps recording. The specific data capture process is as follows. When a call comes in, the user clicks the accept button and picks up the smartphone to answer it. We define the action of pressing the accept button as the first trigger. The earpiece speaker starts playing the sensing signal when the trigger action is performed. When we place the smartphone on the ear, it is the second trigger action. We use acoustic sensing to extract ear-related acoustic features to distinguish users. Then the sensing process is over.

Research shows that the upper frequency of the hearing range for adults is often closer to 15–17kHz [27]. The sampling rate supported on most smartphones can up to 48kHz [28]. According to the Nyquist sampling theorem [29], the maximum frequency of the sensing signal should be less than 24kHz. To achieve wider sensing range and less annoyance, we choose a 25-millisecond chirp signal ranging from 17kHz to 23kHz as our sensing signal, which is a common range for acoustic sensing [30]. We also use a Hamming window [31] to fade at the start and end of the sensing signal, which lowers the acoustic annoyance. Fig. 4 shows an example of the designed sensing signal.

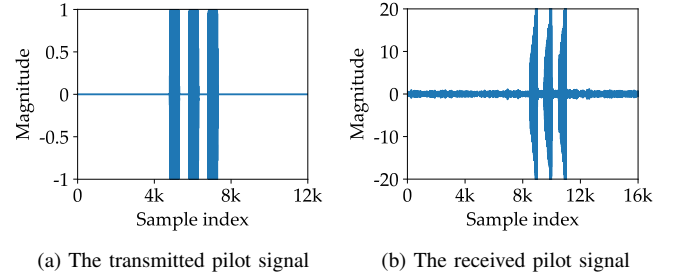


Fig. 5. An example of the pilot signal.

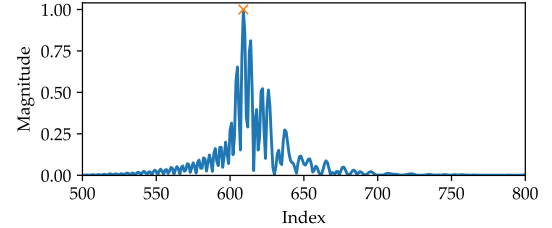


Fig. 6. An example of the cross-correlation result.

#### V. DATA PREPROCESSING

In this section, we introduce the process of signal synchronization, denoising, and signal segmentation.

##### A. Signal Synchronization and Denoising

To eliminate the impact of different system delays, we perform time synchronization between the smartphone speaker and microphone by adding the pilot signal before the sensing signal [32]. Specifically, it contains three chirp signals sweeping from 22kHz to 18kHz. Fig. 5(a) shows an example of the transmitted pilot signal. The received signal is shown in Fig. 5(b). Through signal synchronization, we can accurately locate the start time of the sensing process. The length of one sensing process is 50 milliseconds.

To prevent the received signal from being buried in the noises, we use a Butterworth bandpass filter to remove the out-band noises [33]. Specifically, the frequency range of our sensing signal is from 17kHz to 23kHz. In this way, we get the synchronized signal and eliminate the impact of ambient out-band noises. The output signal is then used for signal segmentation.

##### B. Signal Segmentation

To get ear-related signals, we first select the reference segment and analyze the absolute difference over different segments. For each segment, we then use cross-correlation to better locate the target reflection area.

We set the first signal segment after clicking the accept button as our reference segment. During this quick action, the smartphone is relatively static and is not put on the ear. This reference segment has two functions. One is to be used as a template for the direct path signal. Due to the hardware manufacturing imperfections, the direct path signal will also have uneven attenuation. By doing so, we do not need to put

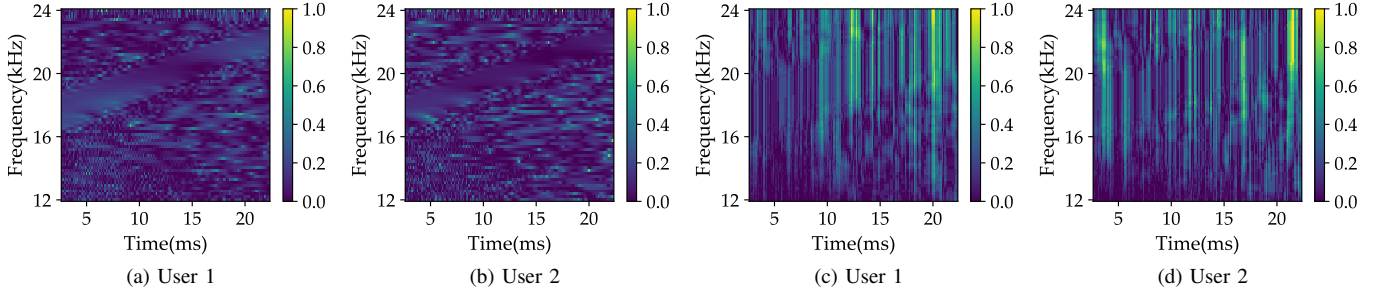


Fig. 7. Normalized magnitude and phase spectrograms for two users. (a) A magnitude spectrogram for user 1. (b) A magnitude spectrogram for user 2. (c) A phase spectrogram for user 1. (d) A phase spectrogram for user 2.

the smartphone in a quiet environment and perform additional detection for the direct path signal. The other is to be used for the elimination of interference factors. The reference segment presents sensing results for humans and the environment. After the smartphone is placed on the ear, we think it is the ear's echoes that mainly cause the change in the received signal. Therefore, we use the absolute difference between different segments to extract ear features later.

Each signal segment contains both direct path signals and reflection signals. We apply each segment to the matched filter to decide the arrival time of the transmitting signal [34]. We calculate the cross-correlation  $R_{xy}$  between the received signal segment  $y(t)$  and the sending sensing signal  $x(t)$  as Eq. 1.

$$R_{xy} = y(t) * x^*(-t) \quad (1)$$

where  $*$  is the convolution operator,  $x^*(-t)$  is the complex conjugate of  $x(-t)$ . As shown in Fig. 6, the highest peak of the cross-correlation result represents the signal traveling directly from the speaker to the microphone. We determine the index with the highest correlation as the start point of our target reflection area since it is impossible for an echo to occur before the direct signal. Finally, we derive a 1200-sample segment as our target signal for feature extraction.

## VI. FEATURE EXTRACTION

In this section, we first perform spectrogram analysis to get normalized spectrograms. Then we use a pre-trained convolution neural network model to extract the representative and robust features.

### A. Spectrogram Analysis

After getting the target reflection area of the signal segment, we use Short-Time Fourier Transform (STFT) to extract the two-dimensional spectrograms for both magnitude and phase features. Since we focus on the high frequency, we retain only the signal components whose frequency is higher than a certain frequency  $f_{start}$  to reduce the computation overhead. We also compute the absolute difference matrix between two spectrograms to eliminate interferences and extract ear-related features. Finally, we perform min-max normalization to get normalized spectrograms.

Specifically, we perform STFT [35] by dividing the target signal into overlapping segments with a fixed sliding window,

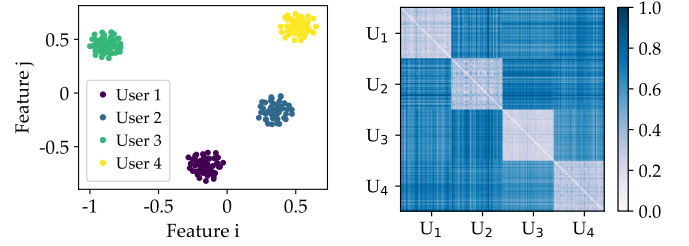


Fig. 8. t-SNE visualization of features for four different users.

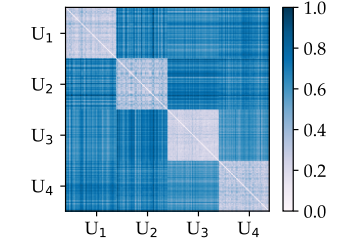


Fig. 9. Euclidean distance between the CNN-based features of four users.

and applying the Fast Fourier Transform (FFT) to these segments. We calculate the magnitude spectrogram  $\mathbf{S}_m$  and the phase spectrogram  $\mathbf{S}_p$ , respectively. They represent the signal's magnitude or phase varying over time and frequency. We then save magnitude and frequency spectrogram with a certain high frequency, i.e.,  $\mathbf{Spec}_m = \mathbf{S}_m(M_{start} :, :)$ , and  $\mathbf{Spec}_p = \mathbf{S}_p(M_{start} :, :)$ . The saved spectrogram is  $\mathbf{Spec} = [\mathbf{Spec}_m; \mathbf{Spec}_p]$ . Then we calculate the absolute difference matrix between the two spectrograms via Eq. 2.

$$\Delta \mathbf{Spec} = |\mathbf{Spec}_s - \mathbf{Spec}_r| \quad (2)$$

where  $\mathbf{Spec}_r$  is the saved spectrogram of the reference segment, and  $\mathbf{Spec}_s$  is the spectrogram of the sensing segment. Then, we perform min-max normalization [36] to normalize the absolute difference matrix  $\Delta \mathbf{Spec}$ , which scales data to the range of [0, 1]. The normalized absolute difference matrix  $\Delta \mathbf{Spec}_{norm}$  can be computed based on Eq. 3.

$$\Delta \mathbf{Spec}_{norm} = \frac{\Delta \mathbf{Spec} - \min(\Delta \mathbf{Spec})}{\max(\Delta \mathbf{Spec}) - \min(\Delta \mathbf{Spec})} \quad (3)$$

In this work, we empirically set  $f_{start}$  as 12 kHz. The sampling rate is set as  $f_s = 48\text{kHz}$  and FFT points is  $N_{fft} = 256$ , so the  $M_{start}$  is  $\frac{f_{start} \times N_{fft}}{f_s} = 64$ . We finally get a size of  $65 \times 158 \times 2$  spectrogram.

As an example, we show two users' normalized magnitude and phase spectrograms in Fig. 7. We can see that spectrograms show differences for different users. These spectrograms are later used as inputs for model training. To visually demonstrate the effectiveness of the spectrograms, we randomly select 200 spectrograms from four different users and use t-Distributed Stochastic Neighbor Embedding (t-SNE) to reduce the dimension [37]. Fig. 8 shows that spectrograms from



TABLE I  
THE STRUCTURE OF OUR BASE CNN MODEL.

Layer	Layer type	Output shape	# Param
1	Conv2D + ReLU	(63,156,16)	304
2	Conv2D + ReLU	(61,154,16)	2,320
3	Max Pooling	(30,77,16)	0
4	Dropout	(30,77,16)	0
5	Conv2D + ReLU	(28,75,32)	4,640
6	Conv2D + ReLU	(26,73,32)	9248
7	Max Pooling	(13,36,32)	0
8	Dropout	(13,36,32)	0
9	Conv2D + ReLU	(11,34,16)	4,624
10	Conv2D + ReLU	(9,32,16)	2,320
11	Max Pooling	(4,16,16)	0
12	Dropout	(4,16,16)	0
13	Flatten	(1024)	0
14	Dense + ReLU	(128)	131,200
15	Dropout	(128)	0
16	Dense + Softmax	(30)	3,870

different users are visually clustered after dimension reduction, which indicates the feasibility of feature extraction.

### B. CNN-based Feature Learning

A significant challenge is the variability in the relative position between the smartphone and the ear during daily usage, leading to a potential decrease in the accuracy of authentication. To address this issue, we propose a VGG-like deep neural network model as a feature extractor to capture representative and robust features, enabling EarPass to handle posture and position variability. Specifically, we utilize transfer learning [38] by removing the last layer of the model and using the middle layer (15<sub>th</sub> layer in Table I) output as the representative features. This approach enables EarPass to extract essential features and maintain accuracy even in cases of posture and position variability.

Table I shows the structure of our base CNN model. Our CNN model contains multiple convolutional layers. We use the rectified linear unit (ReLU) as the activation function for two-dimensional convolution (Conv2D) layers, which mitigates the vanishing gradient problem. The max-pooling layer is used to down-sample the data from the previous activation layer. It reduces the data dimension and saves computational costs. Dropout layers are added after the max-pooling layer to prevent over-fitting. The last layer is the dense layer with a softmax activation function, which outputs the probability of each class. We use categorical cross-entropy as the loss function to train the model. Specifically, the kernel size of the Conv2D and max pooling layers is set as  $3 \times 3$  and  $2 \times 2$ , respectively. The whole model contains 158,526 parameters. The size of the feature extractor is 659 kB, which is available for mobile devices. Finally, we extract a 128-dimensional feature vector, which is utilized in each authentication process.

To test the effectiveness of the CNN-based features, we randomly select 200 testing samples from four users. We then extract CNN-based features from these samples and compare the Euclidean distance between them. Fig. 9 shows the Euclidean distance of four users' extracted CNN-based features. The x-axis and y-axis represent the feature points for four users, and the intersections represent the normalized

euclidean distance. Lighter colors indicate smaller Euclidean distances, while darker colors signify larger distances. The experiment results indicate that the extracted features exhibit high similarity for the same user and low similarity for different users. This observation shows the effectiveness of the feature in distinguishing between users.

## VII. AUTHENTICATION WITH CLASSIFIERS

The training dataset in our scenario exclusively consists of samples from the legitimate call receiver. Therefore, it can be considered a one-class classification problem, commonly known as a novelty detection problem. We utilize data samples from the legitimate user to train a classifier, employing the feature vectors extracted from the CNN-based model. Subsequently, we assess whether the call receiver is legitimate based on the classifier's judgment. We consider two standard novelty detection methods to classify users: one-class support vector machine (OCSVM) [39] and local outlier factor (LOF) [40].

## VIII. DATA COLLECTION

To collect the experiment data, we develop an Android data collection app. We use the earpiece speaker to send inaudible sensing signals and the top microphone as the receiver. After receiving approval from our university's institutional review board (IRB), we started our data collection. We recruited 37 participants, aged from 20 to 27 (graduate and undergraduate students), including 15 males and 15 females. We explicitly informed the participants that the purpose of the experiments was to authenticate the receiver of a call. Similar to answering a call, participants were required to click the start button and picked up the smartphone toward their ear. They were allowed to make slight adjustments to the smartphone's position to cover different situations. In our data collection, we compiled the following 8 datasets.

**Dataset-1.** This dataset is used to train our CNN-based feature extraction model. We recruited 30 participants to collect acoustic signals on Google Pixel 3a. For each of them, we collected 500 acoustic signals. In total, we collected  $30 \times 500 = 15,000$  acoustic signals for CNN model training.

**Dataset-2.** This dataset is utilized to evaluate the overall performance of our system, which is collected under basic settings. We collected acoustic sensing data from 30 participants on Google Pixel 3a. Participants were seated naturally in a quiet environment. We collected 500 acoustic signals for each participant. Besides, we collected acoustic sensing data from 7 unseen participants to evaluate the performance of the CNN-based feature extraction model for new users. We collected 500 acoustic signals for each new participant.

**Dataset-3.** To evaluate the performance of continuous authentication, we collected acoustic sensing data from two situations: listening and speaking. Therefore, we recruited 5 participants and performed acoustic sensing every 1s. We collected 600 acoustic signals for each participant while they were solely listening and another 600 acoustic signals while they were speaking. In total, we collected  $5 \times 600 \times 2 = 6,000$  acoustic signals for dataset-3.

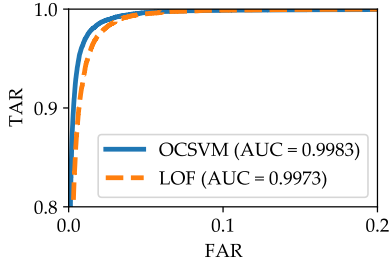


Fig. 10. ROC curves of two classifiers with the best parameters.

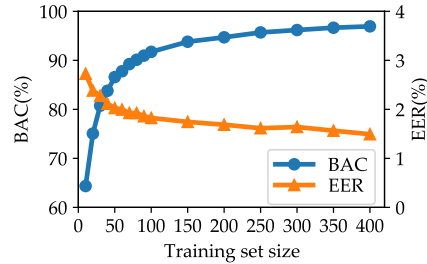


Fig. 11. The BAC and EER for different training set sizes.

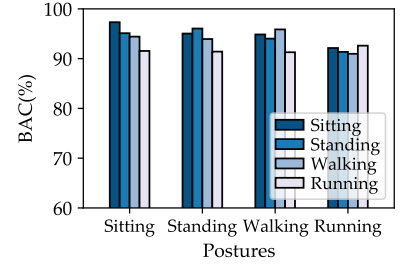


Fig. 12. The BAC of EarPass trained and evaluated under different postures.

**Dataset-4.** To evaluate the influence of ambient noises, we use a laptop as the noise source to simulate the noisy environment. The laptop played the song 'Human Sound/Restaurant2' at 50% volume, which contains common noises in daily life. The sound pressure in this noise environment is about 60-62dB. 30 participants performed this experiment. We collected 500 acoustic signals for each participant in the noisy environment. Dataset-4 involves  $30 \times 500 = 15,000$  acoustic signals.

**Dataset-5.** To evaluate the authentication performance over time, we collected data from different time periods. Dataset-2 is collected in the first round of collection. For 30 participants, we collected data one week and two weeks after the first collection round. For each round of collection, the acoustic signals are  $30 \times 500 = 15,000$ . We finally got 30,000 acoustic signals for dataset-5.

**Dataset-6.** To evaluate the influence of human postures, we consider four common postures: sitting, standing, walking, and running. Dataset-2 was collected under the sitting posture. In this dataset, we recruited 10 participants and collected acoustic data for standing, walking, and running postures. For each participant, we collected 250 acoustic signals for each posture. Finally, we obtained  $10 \times 3 \times 250 = 7,500$  acoustic signals.

**Dataset-7.** To evaluate the performance of our system on different devices, we collected acoustic data on two extra smartphones: Google Pixel 4 and Vivo S12. 10 participants are recruited to do this experiment. For each participant, we collected 500 acoustic signals on each device. As a result, we got  $10 \times 2 \times 500 = 10,000$  acoustic signals for dataset-7.

**Dataset-8.** To evaluate the system defense against attacks, we chose 7 participants to serve as attackers. Then we evaluated two types of attacks: zero-effort attack and mimicry attack. i) Dataset-8A. For the zero-effort attack, 7 participants attempted to guess how the legitimate user performs the authentication process. We finally got  $7 \times 500 = 3,500$  acoustic signals on Google Pixel 3a for dataset-8A. ii) Dataset-8B. For the mimicry attack, the attacker observes and imitates the authentication process of legitimate users. Specifically, each attacker chose 5 participants to carefully observe and then imitate their authentication process. We finally got  $7 \times 500 = 3,500$  acoustic signals on Google Pixel 3a for dataset-8B.

## IX. EVALUATION

In this section, we report the evaluation results of the proposed system. We first present the evaluation metrics, and

show the system performance of EarPass. Additionally, we evaluate its effectiveness under different settings and security against attacks. Finally, we present the authentication latency of our system.

### A. Evaluation Metrics

There are four possible results of classification: True acceptance (TA), True rejection (TR), False acceptance (FA), False rejection (FR). We use the following metrics to evaluate the performance of EarPass. True acceptance rate is defined as  $TAR = \frac{TA}{TA+FR}$ , which measures the proportion of samples classified as positive among legitimate user samples. True rejection rate is defined as  $TRR = \frac{TR}{TR+FA}$ , which measures the proportion of samples classified as negative among illegal user samples. Balanced accuracy (BAC) is the average of true acceptance rate and true rejection rate, which is defined as  $BAC = \frac{1}{2}(TAR + TRR)$ . It is used to evaluate the accuracy of imbalanced datasets. A higher BAC means better performance of the system. False acceptance rate ( $FAR = \frac{FA}{FA+TR}$ ) represents the rate at which illegal samples are wrongly accepted. False rejection rate ( $FRR = \frac{FR}{FR+TA}$ ) represents the rate at which legitimate samples are wrongly rejected. Receiver operation characteristic (ROC) shows dynamic changes of TAR against FAR at different classification thresholds. The area under the ROC curve (AUC) is used to measure the probability that prediction scores of legitimate users are higher than illegal users. Equal error rate (EER) is the point on the ROC curve, where FAR is equal to FRR. A larger AUC and lower EER mean better performance of the system.

### B. System Performance

**Authentication accuracy.** We use 30 users in dataset-2 to evaluate the authentication effectiveness of EarPass. We employ a 5-fold cross-validation for each user to split the data and train a one-class classifier. Then we test the classifier model using the remaining data of the user as well as data from other users.

This study considers two types of one-class classifiers: one-class support vector machine (OCSVM) and local outlier factor (LOF). Parameters such as the *kernel*,  $\gamma$ , and  $\nu$  significantly impact the results for OCSVM, while for LOF, we consider the  $n_n$  neighbors parameter. We employ grid search to find the best parameter combinations for each classifier. Ultimately, we determine that the radial basis function kernel works best for

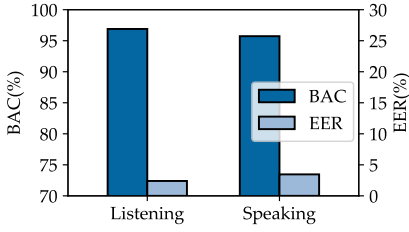


Fig. 13. The BAC and EER performance for continuous authentication.

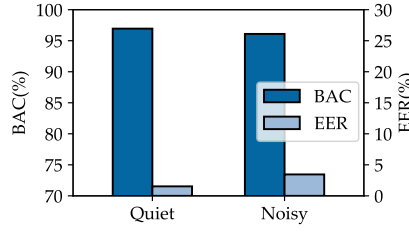


Fig. 14. The BAC and EER performance under different noise conditions.

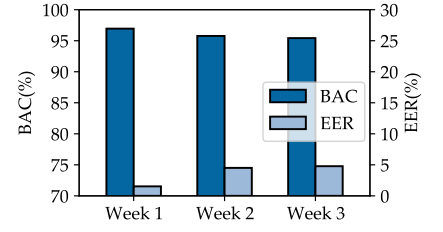


Fig. 15. The BAC and EER performance at different time periods.

TABLE II  
MEAN/STANDARD DEVIATION OF BAC(%), EER(%), AND AUC UNDER TWO DIFFERENT ONE-CLASS CLASSIFIERS.

Classifier	Mean/Std BAC	Mean/Std EER	Mean/Std AUC
OCSVM	96.95/1.45	1.53/1.35	0.9982/0.0025
LOF	96.13/3.18	1.90/1.56	0.9972/0.0034

TABLE III  
MEAN/STANDARD DEVIATION OF BAC(%), EER(%), AND AUC FOR NEW USERS.

Classifier	Mean/Std BAC	Mean/Std EER	Mean/Std AUC
OCSVM	96.48/1.63	2.78/1.95	0.9955/0.0043
LOF	93.49/4.59	2.89/2.21	0.9946/0.0063

OCSVM, with  $\gamma = \text{'scale'}$  and  $\nu = 0.01$ . For LOF, the optimal  $n_{neighbors}$  value is 3. Fig. 10 presents the ROC curves of the two classifiers with the best parameters. The AUC for OCSVM is 0.9983, and for LOF, it is 0.9973. A higher AUC value suggests better system performance. The results indicate that the OCSVM classifier outperforms the LOF classifier. Table II shows the mean and standard deviation of BAC, EER, and AUC metrics under two classifiers. OCSVM demonstrates superior BAC and EER metrics compared to LOF, thus we select it as our classifier for subsequent evaluations. This experiment reveals that EarPass achieves an average BAC of 96.95% and an EER of 1.53% using the OCSVM classifier. These results indicate that EarPass is effective in distinguishing users.

To evaluate the performance of EarPass on 30 different users, we show the BAC of each user in Fig. 16. The best case of the 30 users is user 25, and the BAC is 98.5%. Although the performance of EarPass varies for each user, the BAC for all users exceeds 95%, indicating the effectiveness of EarPass.

**Performance on new user.** To evaluate the performance of the CNN-based feature extractor on new users, we use the data from 7 unseen participants in dataset-2, which is not used for CNN training. We use 5-fold cross-validation to split the data. Then we train a one-class SVM (OCSVM) classifier and a local outlier factor (LOF) classifier for each participant. Table III shows the mean and standard deviation of BAC, EER, and AUC metrics for new users under two classifiers. The BACs for OCSVM and LOF are 96.48% and 93.49%, respectively. Compared to results in Table II, the BAC falls 0.47% for OCSVM and falls 2.64% for LOF. For the OCSVM classifier, the BAC is over 96%, demonstrating the feature extractor's effectiveness for new users. Although the feature extractor is trained on limited data, it is still available

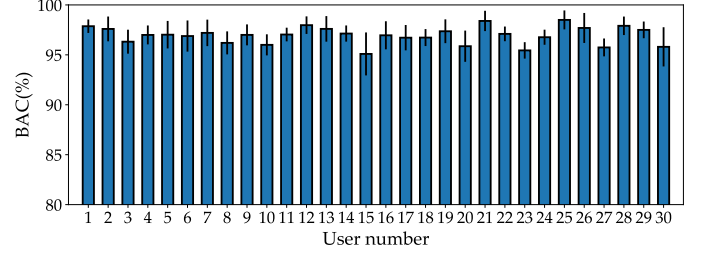


Fig. 16. BAC performance for each user.

to a wide range of users.

**Impact of training dataset size.** To investigate the impact of training set size, we change the amount of training data points for each user on dataset-2. Specifically, for each user, we vary the training data points from 10 to 400 in steps of 10 or 50 to train a one-class SVM classifier. Then we test on the rest of the data. Fig. 11 shows the BAC and EER for different training set sizes. As the size of the training set increases from 10 to 400, the BAC rises from 64.35% to 96.94%. The EER falls to 1.49% from 2.73% when the training set size increases from 10 to 400. That may be because the classifier can learn a better boundary with more legitimate data. The BAC is over 90% with 80 training data points and is over 95% with 200 training data points. With 50 training data points, the EER is less than 2%. These results show that our system is practical on mobile devices.

**Performance of continuous authentication.** We analyze two common situations to evaluate the performance of continuous authentication. During the process of answering a call, the receiver will be in one of two states: listening to the caller or speaking to the caller. We train on dataset-2 and test on dataset-3 for evaluation. The results are shown in Fig. 13. For listening and speaking states, the BACs are 96.89% and 95.73%, respectively. The EERs are 2.39% and 3.46%, respectively. The comparison shows that the listening state's performance is better than the speaking state's. That may be because there is a slight change in the outer ear when speaking. In total, the experimental results show that EarPass is available for continuous authentication.

### C. Impact Factors Study

**Impact of ambient noise.** To find out the impact of ambient noises on acoustic sensing, we compare the system performance under different noise conditions. In this experiment,



TABLE IV  
MEAN/STANDARD DEVIATION OF BAC(%), EER(%), AND AUC FOR  
THREE DIFFERENT DEVICES.

Classifier	Mean/Std BAC	Mean/Std EER	Mean/Std AUC
Pixel 3a	97.32/1.55	0.85/0.80	0.9994/0.0011
Pixel 4	97.62/1.47	0.86/1.29	0.9989/0.0027
Vivo S12	95.20/1.19	4.03/1.02	0.9926/0.0036

TABLE V  
BYPASSED SAMPLES, FAR(%) AND MEAN PREDICTION SCORES UNDER  
TWO DIFFERENT ATTACKS.

Attack	Bypassed samples	FAR	Prediction scores
Zero-effort attack	33(3500)	0.94	-0.39
Mimicry attack	49(3500)	1.40	-0.42

we use dataset-2 for training, which is collected in a quiet environment. Then we test on dataset-2 and dataset-4 to evaluate the performance. Fig. 14 shows BACs and EERs in quiet and noisy environments respectively. The BAC is 96.95% in a quiet environment and falls 0.86% in a noisy environment, which is 96.09%. The EER is 1.53% in a quiet environment and rises 1.92% in a noisy environment, which is 3.45%. There is still a high BAC and low EER in a noisy environment, demonstrating that EarPass is robust to ambient noises.

**Performance over time.** We collected data at three different periods to evaluate the system’s performance over time. In this experiment, we use dataset-2 for training, and test on dataset-2 and dataset-5. Specifically, the data in dataset-2 is collected in the first week, and the data collected in the following two weeks is in dataset-5. Fig. 15 shows the BACs and EERs for different weeks. For week 2 and week 3, the BACs are 95.77% and 95.42%. The EERs are 4.51% and 4.78% for week 2 and week 3. We set week 1 as the reference. For week 2 and week 3, the BACs have slight drops of 1.18% and 1.53%. This may be caused by slight changes in the user’s posture when holding the device. To address this issue, EarPass can be designed to update the authentication model using newly collected data, which is known as the model updating mechanism [41].

**Impact of different postures.** To evaluate the impact of different postures, we use 10 participants’ data in dataset-2 and dataset-6. The data in dataset-2 is collected when the participant is sitting. Dataset-6 contains data on standing, walking, and running. We take turns selecting one posture for training and testing the other postures for each participant. For example, we train on sitting posture data and test on sitting, standing, walking, and running posture data. Similarly, we train on the other three postures. Fig. 12 shows the BAC of EarPass under different postures. For example, when we use sitting data for training and testing on the rest of the data, the BACs for the four postures are 97.28%, 95.11%, 94.43%, and 91.55%, respectively. As we can see, when the posture of training and testing is the same, the BAC is the highest. The results also show that EarPass performs better in sitting, standing, and walking postures than in the running. It is relatively rare to answer the phone while running. If we ignore ‘running’, EarPass achieves over 94% BAC for other postures, which shows EarPass applies to multiple postures.

**Impact of different devices.** We collected data on three

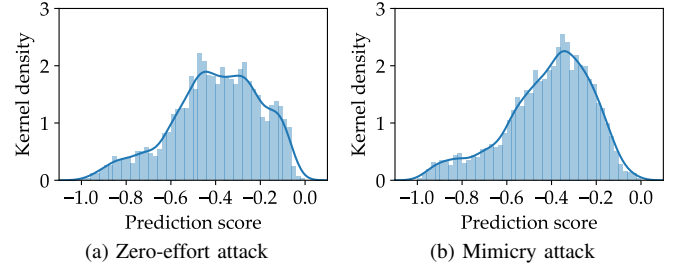


Fig. 17. The kernel density of attack dataset’s prediction score.

smartphones to evaluate the system performance on different devices. In this experiment, we use dataset-2 and dataset-7 for evaluation. Dataset-2 is collected on Google Pixel 3a. Data collected on Google Pixel 4 and Vivo S12 is in dataset-7. We train the one-class SVM classifier for each user on a different smartphone. As shown in Table IV, the mean BACs on Pixel 3a, Pixel 4, and Vivo S12 are 97.32%, 97.62%, and 95.20%, respectively. The average EERs on Pixel 3a, Pixel 4, and Vivo S12 are 0.85%, 0.86%, and 4.03%, respectively. The worst performance is on Vivo S12, which may be caused by hardware imperfection. Despite this, the BAC of Vivo S12 is over 95%, which indicates the effectiveness of our system on different devices.

#### D. Evaluation of Attack Resistance

To evaluate the system security against two different attacks, we use dataset-8A and dataset-8B to test the authentication model trained using dataset-2. We use FAR as the rate of wrongly accepted illegal samples in this evaluation. We also investigate the distribution and kernel density of the attack dataset’s prediction scores, which are evaluated under the Gaussian kernel.

Table V shows the result of bypassed samples, FAR(%), and mean prediction scores under two types of attacks. We test 3500 illegal samples for the zero-effort attack, 33 of which are wrongly accepted. For the zero-effort attack, the FAR is 0.94%, and the mean prediction score is -0.39. We also test on 3500 illegal samples for the mimicry attack, where the number of bypassed samples is 49. For the mimicry attack, the FAR is 1.40%, and the mean prediction score is -0.42. These results demonstrate that EarPass can defend against these two attacks. The distribution and kernel density of the two attacks’ prediction scores are shown in Fig. 17. Specifically, Fig. 17 (a) shows the prediction scores’ distribution under zero-effort attack using dataset-8A. The kernel density shows a wide range but with a low prediction score. Fig. 17 (b) shows the prediction scores’ distribution under mimicry attack using dataset-8B. The kernel density shows a wide range and a lower score than the scores under the zero-effort attack.

#### E. Authentication Latency

We define the authentication latency of our system as the time from recording the received signal to producing the authentication result. Therefore, it consists of time for three modules: data preprocessing, feature extraction, and classification.

TABLE VI  
COMPARISON OF TYPICAL CALL RECEIVER AUTHENTICATION METHODS ON SMARTPHONES

Method	Source of distinctiveness	Authentication before answering	No extra device	Unchanging answering behavior <sup>1</sup>	Non-root authentication <sup>2</sup>	Accuracy	EER
Conti <i>et al.</i> [6]	Arm motion behavior	✓	✓	×	✓	N/A	~ 7%
Answerauth [10]	Arm motion behavior	✓	✓	×	✓	98.98%	N/A
Cherifi <i>et al.</i> [13]	Ear image	✓	✓	×	✓	N/A	5.15%
Barra <i>et al.</i> [12]	Ear image	✓	✓	×	✓	N/A	17.7%
Bodyprint [14]	Ear capacitive image	✓	✓	×	×	99.52%	N/A
EarEcho [16]	Acoustic sensing	×	×	✓	✓	94.52%	N/A
Earmonitor [18]	Acoustic sensing	✓	×	✓	✓	96.4%	N/A
EarPass (our work)	Acoustic sensing	✓	✓	✓	✓	96.95%	1.53%

<sup>1</sup> : Unchanging answering behavior implies that the authentication method does not modify the way users answer calls, nor does it depend on a predetermined call-answering pattern.

<sup>2</sup> : Non-root authentication means that the authentication method does not rely on the root privilege to authenticate users.

We developed a prototype system named EarPass on Android to evaluate the authentication latency. We evaluate one sensing process and compute the average latency from 50 tries. On Google Pixel 3a, the average authentication latency for the three modules is 82.8ms, 57.6ms, and 69.6ms, respectively. In total, EarPass requires 0.21s to complete authentication.

## X. RELATED WORK

In this section, we present related works about call receiver authentication and acoustic sensing.

### A. Call Receiver Authentication

Authenticating the identity of the call receiver is crucial for ensuring the security and privacy of voice communication, where the goal is to guarantee that only the legitimate user can answer the call. Researchers have attempted to address this problem through the following two types of solutions: behavioral characteristics and physiological characteristics. Table VI summarizes some typical call receiver authentication methods on smartphones.

**Behavioral characteristics.** Behavioral characteristics of call answering have been extensively explored for distinguishing the call receiver [6]–[11]. These methods primarily focus on unique arm movement features exhibited during call answering by users. They rely on motion sensors to capture device movements and analyze the arm motion behavior of picking up the smartphone when accepting a call to verify whether the user is authorized. However, users’ behavior is variable and uncontrollable [19]. These methods require users’ authentication behavior to follow fixed patterns, which makes these systems prone to more false rejections by the system.

**Physiological characteristics.** Researchers have also explored the use of physiological features of the ear to distinguish users. Typically, short video sequences when approaching the ear are often employed for ear-based call receiver authentication [12], [13]. However, these methods are sensitive to the environmental conditions, such as low light intensity. They require users to make extra gestures to obtain a clearer ear image, which can be inconvenient. Touchscreen has also been utilized as a capacitive sensor to capture the capacitive image of a user’s ear for authentication [14], [15]. However, not all areas on the screen may effectively capture capacitive values, necessitating users to position their ear correctly. Besides,

these methods require rooting the smartphone and modifying the touchscreen module in the kernel source, which could compromise the integrity of the smartphone. Some methods also utilize acoustic signals to sense the ear [16]–[18], while relying on extra devices, e.g., wireless earphones. Besides, EarEcho [16] uses call audios to sense the ear canal. However, authentication occurs after answering a call, which does not guarantee that only authorized users can access the call. Mahto *et al.* [17] employ audible signals for sensing, which may interfere with users. Our method provides protection before the call is answered, does not require extra devices, and imposes no additional burdens on users.

### B. Acoustic Sensing

Acoustic sensing has attracted significant attention and been applied in many fields nowadays. By exploiting speakers and microphones, it can be utilized to sense the environment [42]–[44], human behaviors such as hand tracking [45]–[49], lip reading [50]–[53], and breathing monitoring [54], [55], as well as human physiological biometrics including hand [25], [28], [56]–[58], face [59]–[62], and ear [16]–[18].

Ren *et al.* [42] use ambient noises for proximity detection. Cai *et al.* [43] utilize dual microphones to estimate air-borne sound propagation speed, thereby deriving ambient temperature. Echotrack [45] uses the chirp’s time of flight to measure the distance from the hand to the speaker, and then the hand can be located with triangular geometry. VSkin [46] uses both the structure-borne and air-borne sounds to achieve gesture sensing on the back of mobile devices. Lu *et al.* [50] leverage the smartphone as a Doppler sonar to extract unique behavioral characteristics of users’ speaking lips for authentication. Echo-Hand [28] complements camera-based 2-dimensional hand geometry recognition of one hand with active acoustic sensing of the other hand. EchoPrint [59] enhances the security of face authentication against representation attacks by emitting inaudible acoustic signals and extracts 3D Face related features from the echoes. Mahto *et al.* [17] employ audible signals for authentication. EarEcho [16] requires users to answer the calls first and then authenticates users. Our work uses the inaudible acoustic signal to sense the outer ear without interfering with the normal voice conversation. It authenticates the call receiver implicitly and does not need extra devices.

## XI. DISCUSSION

In this section, we discuss some limitations in our work and experiments, and outlook for potential improvements in future work. Our study focuses on sensitive private calls. For the sake of security, our method works on the earpiece mode, which means users put the smartphone close to ear to answer the call. We do not cover all answering scenarios, such as the use of additional devices to assist in answering, like wireless earphones. EarPass may reject a legitimate user if he uses one ear to register while the other ear is used for authentication. In the next version, we plan to extend EarPass to support authentication with two ears and multiple legitimate users. While our CNN-based feature extractor has been designed to capture robust features under variable positions during call answering for the same subject, we acknowledge that EarPass may reject the legitimate user if there are significant changes in position. In future work, we will conduct additional experiments to investigate the specific effects of position on EarPass. A user's device-holding style may change over time, leading to variability in the relative position between the smartphone and the ear, which could result in a higher false rejection rate over a longer time. One possible solution is to implement a model updating mechanism, i.e., updating the authentication model using newly collected data points. Additionally, the current CNN-based feature extractor is pre-trained on limited user data, and to improve performance in various conditions, we may need to train on a larger scale of data. Furthermore, we plan to measure system performance, such as power consumption, on various smartphone platforms to ensure optimal performance.

## XII. CONCLUSION

In this paper, we propose EarPass, a secure and implicit call receiver authentication scheme on smartphones. EarPass utilizes representative acoustic characteristics for authentication without necessitating special hardware or additional operations. Specifically, it leverages the earpiece speaker to emit the inaudible sensing signal and the top microphone to record echoes. A CNN-based feature extractor handles the issue of posture and position variability, and a one-class classifier determines the legitimacy of the user. Experimental results demonstrate that EarPass achieves a 96.95% balanced accuracy and a 1.53% equal error rate. Furthermore, it exhibits resilience against potential attacks. EarPass can be extended to other voice scenarios, such as private voice messages, thereby significantly enhancing the security of voice-related authentication problems.

## REFERENCES

- [1] "Whatsapp," <https://www.whatsapp.com/>.
- [2] "Wechat - free messaging and calling app," <https://www.wechat.com/en/>.
- [3] "Dingtalk, make work and study easy," <https://www.dingtalk.com/en>.
- [4] B. Reaves, L. Blue, H. Abdullah, L. Vargas, P. Traynor, and T. Shrimpton, "Authenticall: Efficient identity and content authentication for phone calls," in *USENIX Security Symposium*, 2017.
- [5] C. Du, H. Yu, Y. Xiao, Y. T. Hou, A. D. Keromytis, and W. Lou, "Ucblocker: Unwanted call blocking using anonymous authentication," in *USENIX Security Symposium*, 2023.
- [6] M. Conti, I. Zachia-Zlatea, and B. Crispo, "Mind how you answer me! transparently authenticating the user of a smartphone when answering or placing a call," in *ACM Asia Conference on Computer and Communications Security (AsiaCCS)*, 2011.
- [7] A. Eremin, K. Kogos, and Y. Valatskayte, "Touch and move: Incoming call user authentication," in *International Conference on Information Systems Security and Privacy (ICISSP)*, 2019.
- [8] A. Buriro, B. Crispo, F. D. Frari, J. Klardie, and K. Wrona, "Itsme: Multi-modal and unobtrusive behavioural user authentication for smartphones," in *International Conference on Passwords (PASSWORDS)*, 2015.
- [9] W.-H. Lee, X. Liu, Y. Shen, H. Jin, and R. B. Lee, "Secure pick up: Implicit authentication when you start using the smartphone," in *ACM Symposium on Access Control Models and Technologies (SACMAT)*, 2017.
- [10] A. Buriro, B. Crispo, and M. Conti, "Answerauth: A bimodal behavioral biometric-based user authentication scheme for smartphones," *Journal of information security and applications (JISA)*, 2019.
- [11] B. Fan, X. Su, J. Niu, and P. Hui, "Emgauth: Unlocking smartphones with emg signals," *IEEE Transactions on Mobile Computing (TMC)*, 2022.
- [12] A. F. Abate, M. Nappi, and S. Ricciardi, "Smartphone enabled person authentication based on ear biometrics and arm gesture," in *IEEE International Conference on Systems, Man and Cybernetics (SMC)*, 2016.
- [13] F. Cherifi, K. Amroun, and M. Omar, "Robust multimodal biometric authentication on iot device through ear shape and arm gesture," *Multimedia Tools and Applications (MTA)*, 2021.
- [14] C. Holz, S. Buthpitiya, and M. Knaust, "Bodyprint: Biometric user identification on mobile devices using the capacitive touchscreen to scan body parts," in *ACM Conference on Human Factors in Computing Systems (CHI)*, 2015.
- [15] M. A. Rilvan, K. I. Lacy, M. S. Hossain, and B. Wang, "User authentication and identification on smartphones by incorporating capacitive touchscreen," in *IEEE International Performance, Computing, and Communications Conference (IPCCC)*, 2016.
- [16] Y. Gao, W. Wang, V. V. Phooha, W. Sun, and Z. Jin, "Earecho: Using ear canal echo for wearable authentication," *Proceedings of the ACM on Interactive, Mobile, Wearable and Ubiquitous Technologies (IMWUT)*, 2019.
- [17] S. Mahto, T. Arakawa, and T. Koshinak, "Ear acoustic biometrics using inaudible signals and its application to continuous user authentication," in *European Signal Processing Conference (EUSIPCO)*, 2018.
- [18] X. Sun, J. Xiong, C. Feng, W. Deng, X. Wei, D. Fang, and X. Chen, "Earmonitor: In-ear motion-resilient acoustic sensing using commodity earphones," *Proceedings of the ACM on Interactive, Mobile, Wearable and Ubiquitous Technologies (IMWUT)*, 2023.
- [19] C. Wu, H. Cao, G. Xu, C. Zhou, J. Sun, R. Yan, Y. Liu, and H. Jiang, "It's all in the touch: Authenticating users with host gestures on multi-touch screen devices," *IEEE Transactions on Mobile Computing (TMC)*, 2024.
- [20] A. Abaza, A. Ross, C. Hebert, M. A. F. Harrison, and M. S. Nixon, "A survey on ear biometrics," *ACM Computing Surveys (CSUR)*, 2013.
- [21] X. Sun, J. Xiong, C. Feng, H. Li, Y. Wu, D. Fang, and X. Chen, "Earssr: Silent speech recognition via earphones," *IEEE Transactions on Mobile Computing (TMC)*, 2024.
- [22] C. Wang, F. Lin, T. Liu, K. Zheng, Z. Wang, Z. Li, M.-C. Huang, W. Xu, and K. Ren, "mmeve: eavesdropping on smartphone's earpiece via cots mmwave device," in *ACM Conference on Mobile Computing and Networking (MobiCom)*, 2022.
- [23] B. Reaves, L. Blue, and P. Traynor, "Authloop: End-to-end cryptographic authentication for telephony over voice channels," in *USENIX Security Symposium*, 2016.
- [24] S. Wang, L. Zhong, Y. Fu, L. Chen, J. Ren, and Y. Zhang, "Uface: Your smartphone can hear your facial expression!" *Proceedings of the ACM on Interactive, Mobile, Wearable and Ubiquitous Technologies (IMWUT)*, 2024.
- [25] Y. Yang, Y. Wang, Y. Chen, and C. Wang, "Echolock: Towards low-effort mobile user identification leveraging structure-borne echos," in *ACM Asia Conference on Computer and Communications Security (AsiaCCS)*, 2020.
- [26] C. Cai, R. Zheng, and J. Luo, "Ubiquitous acoustic sensing on commodity iot devices: A survey," *IEEE Communications Surveys & Tutorials*, 2022.
- [27] D. Purves, G. J. Augustine, D. Fitzpatrick, L. C. Katz, and A. S. Lamantia, *Neuroscience, 2nd edition*. Sinauer Associates, 2001.

- [28] C. Wu, J. Chen, K. He, Z. Zhao, R. Du, and C. Zhang, "Echohand: High accuracy and presentation attack resistant hand authentication on commodity mobile devices," in *Conference on Computer and Communications Security (CCS)*, 2022.
- [29] Z. Ba, T. Zheng, X. Zhang, Z. Qin, B. Li, X. Liu, and K. Ren, "Learning-based practical smartphone eavesdropping with built-in accelerometer," in *Network and Distributed System Security Symposium (NDSS)*, 2020.
- [30] Z. Wang, S. Tan, L. Zhang, Y. Ren, Z. Wang, and J. Yang, "Eardynamic: An ear canal deformation based continuous user authentication using in-ear wearables," *Proceedings of the ACM on Interactive, Mobile, Wearable and Ubiquitous Technologies (IMWUT)*, 2021.
- [31] E. C. Ifeachor and B. W. Jervis, *Digital signal processing: a practical approach*. Pearson Education, 2002.
- [32] Y.-C. Tung and K. G. Shin, "Expansion of human-phone interface by sensing structure-borne sound propagation," in *ACM SIGMOBILE International Conference on Mobile Systems, Applications, and Services (MobiSys)*, 2016.
- [33] Y. Xie, F. Li, Y. Wu, H. Chen, Z. Zhao, and Y. Wang, "Teethpass: Dental occlusion-based user authentication via in-ear acoustic sensing," in *IEEE Conference on Computer Communications (INFOCOM)*, 2022.
- [34] J. Chen, U. Hengartner, H. Khan, and M. Mannan, "Chaperone: Real-time locking and loss prevention for smartphones," in *USENIX Security Symposium*, 2020.
- [35] D. Chen, A. B. Wong, and K. Wu, "Fall detection based on fusion of passive and active acoustic sensing," *IEEE Internet of Things Journal*, 2023.
- [36] J. Liu, W. Song, L. Shen, J. Han, and K. Ren, "Secure user verification and continuous authentication via earphone imu," *IEEE Transactions on Mobile Computing (TMC)*, 2022.
- [37] Y. Meng, J. Li, M. Pillari, A. Deopujari, L. Brennan, H. Shamsie, H. Zhu, and Y. Tian, "Your microphone array retains your identity: A robust voice liveness detection system for smart speaker," in *USENIX Security Symposium*, 2022.
- [38] C. Wu, K. He, J. Chen, Z. Zhao, and R. Du, "Liveness is not enough: Enhancing fingerprint authentication with behavioral biometrics to defeat puppet attacks," in *USENIX Security Symposium*, 2020.
- [39] B. Schölkopf, R. Williamson, A. Smola, J. Shawe-Taylor, and J. Platt, "Support vector method for novelty detection," in *Conference on Neural Information Processing Systems (NIPS)*, 1999.
- [40] M. M. Breunig, H.-P. Kriegel, R. T. Ng, and J. Sander, "Lof: identifying density-based local outliers," in *ACM SIGMOD Conference (SIGMOD)*, 2000.
- [41] C. Wu, K. He, J. Chen, Z. Zhao, and R. Du, "Toward robust detection of puppet attacks via characterizing fingertip-touch behaviors," *IEEE Transactions on Dependable and Secure Computing (TDSC)*, 2021.
- [42] Y. Ren, P. Wen, H. Liu, Z. Zheng, Y. Chen, P. Huang, and H. Li, "Proximity-echo: Secure two factor authentication using active sound sensing," in *IEEE Conference on Computer Communications (INFOCOM)*, 2021.
- [43] C. Cai, H. Pu, L. Ye, H. Jiang, and J. Luo, "Active acoustic sensing for "hearing" temperature under acoustic interference," *IEEE Transactions on Mobile Computing (TMC)*, 2021.
- [44] Y. Su, F. Zhang, K. Niu, T. Wang, B. Jin, Z. Wang, Y. Jiang, D. Zhang, L. Qiu, and J. Xiong, "Embracing distributed acoustic sensing in car cabin for children presence detection," *Proceedings of the ACM on Interactive, Mobile, Wearable and Ubiquitous Technologies (IMWUT)*, 2024.
- [45] H. Chen, F. Li, and Y. Wang, "EchoTrack: Acoustic device-free hand tracking on smart phones," in *IEEE Conference on Computer Communications (INFOCOM)*, 2017.
- [46] K. Sun, T. Zhao, W. Wang, and L. Xie, "Vskin: Sensing touch gestures on surfaces of mobile devices using acoustic signals," in *ACM Conference on Mobile Computing and Networking (MobiCom)*, 2018.
- [47] Y. Wang, J. Shen, and Y. Zheng, "Push the limit of acoustic gesture recognition," *IEEE Transactions on Mobile Computing (TMC)*, 2020.
- [48] P. Wang, R. Jiang, and C. Liu, "Amaging: Acoustic hand imaging for self-adaptive gesture recognition," in *IEEE Conference on Computer Communications (INFOCOM)*, 2022.
- [49] H. Cheng and W. Lou, "Pd-fmcw: push the limit of device-free acoustic sensing using phase difference in fmcw," *IEEE Transactions on Mobile Computing (TMC)*, 2022.
- [50] L. Lu, J. Yu, Y. Chen, H. Liu, Y. Zhu, Y. Liu, and M. Li, "Lippass: Lip reading-based user authentication on smartphones leveraging acoustic signals," in *IEEE Conference on Computer Communications (INFOCOM)*, 2018.
- [51] Q. Zhang, D. Wang, R. Zhao, Y. Yu, and J. Shen, "Sensing to hear: Speech enhancement for mobile devices using acoustic signals," *Proceedings of the ACM on Interactive, Mobile, Wearable and Ubiquitous Technologies (IMWUT)*, 2021.
- [52] Y. Fu, S. Wang, L. Zhong, L. Chen, J. Ren, and Y. Zhang, "Voice: enabling voice communication in silence via acoustic sensing on commodity devices," in *ACM International Conference on Embedded Networked Sensor Systems (SenSys)*, 2022.
- [53] R. Zhang, K. Li, Y. Hao, Y. Wang, Z. Lai, F. Guimbretière, and C. Zhang, "Echospeech: Continuous silent speech recognition on minimally-obtrusive eyewear powered by acoustic sensing," in *ACM Conference on Human Factors in Computing Systems (CHI)*, 2023.
- [54] R. Nandakumar, S. Gollakota, and N. Watson, "Contactless sleep apnea detection on smartphones," in *ACM SIGMOBILE International Conference on Mobile Systems, Applications, and Services (MobiSys)*, 2015.
- [55] X. Song, B. Yang, G. Yang, R. Chen, E. Forno, W. Chen, and W. Gao, "Spirosonic: monitoring human lung function via acoustic sensing on commodity smartphones," in *ACM Conference on Mobile Computing and Networking (MobiCom)*, 2020.
- [56] H. Chen, F. Li, W. Du, S. Yang, M. Conn, and Y. Wang, "Listen to your fingers: User authentication based on geometry biometrics of touch gesture," *Proceedings of the ACM on Interactive, Mobile, Wearable and Ubiquitous Technologies (IMWUT)*, 2020.
- [57] M. Zhou, Q. Wang, X. Lin, Y. Zhao, P. Jiang, Q. Li, C. Shen, and C. Wang, "Presspin: Enabling secure pin authentication on mobile devices via structure-borne sounds," *IEEE Transactions on Dependable and Secure Computing (TDSC)*, 2022.
- [58] Y. Yang, X. Li, Z. Ye, Y. Wang, and Y. Chen, "Biocase: Privacy protection via acoustic sensing of finger touches on smartphone case mini-structures," in *ACM SIGMOBILE International Conference on Mobile Systems, Applications, and Services (MobiSys)*, 2023.
- [59] B. Zhou, Z. Xie, Y. Zhang, J. Lohokare, R. Gao, and F. Ye, "Robust human face authentication leveraging acoustic sensing on smartphones," *IEEE Transactions on Mobile Computing (TMC)*, 2021.
- [60] G. Wang, Q. Yan, S. Patrarungrong, J. Wang, and H. Zeng, "Facer: Contrastive attention based expression recognition via smartphone ear-piece speaker," in *IEEE Conference on Computer Communications (INFOCOM)*, 2023.
- [61] P. Kar, S. Singh, A. Mandal, S. Chattopadhyay, and S. Chakraborty, "Expressense: Exploring a standalone smartphone to sense engagement of users from facial expressions using acoustic sensing," in *ACM Conference on Human Factors in Computing Systems (CHI)*, 2023.
- [62] Z. Xu, T. Liu, R. Jiang, P. Hu, Z. Guo, and C. Liu, "Aface: Range-flexible anti-spoofing face authentication via smartphone acoustic sensing," *Proceedings of the ACM on Interactive, Mobile, Wearable and Ubiquitous Technologies (IMWUT)*, 2024.



**Xiping Sun** received the B.E. degree in information security from Wuhan University, China, in 2019. She is currently pursuing the Ph.D. degree with the School of Cyber Science and Engineering, Wuhan University, China. Her research interests include system and mobile security.



**Jing Chen** received the Ph.D. degree in computer science from Huazhong University of Science and Technology, Wuhan. He worked as a full professor in Wuhan University from 2015. He is the deputy Dean of the School of Cyber Science and Engineering at Wuhan University. His research interests in computer science are in the areas of network security, cloud security. He has published more than 100 research papers in many international conferences and journals, such as USENIX Security, CCS, INFOCOM, TDSC, TIFS, TMC, TC, TPDS et al. He acts as

a reviewer for many conferences and journals, such as IEEE INFOCOM, IEEE Transactions on Information Forensics and Security, IEEE Transactions on Dependable and Secure Computing and IEEE/ACM Transactions on Networking.





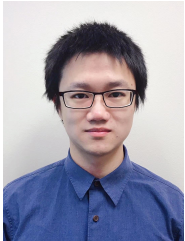
**Kun He** received his Ph.D. from Wuhan University, Wuhan, China. He is currently an associate professor with Wuhan University. His research interests include cryptography and data security. He has published more than 30 research papers in various journals and conferences, such as TIFS, TDSC, TMC, USENIX Security, CCS, and INFOCOM.



**Zhixiang He** received the B.E. degree in communication engineering from Chongqing University of China, China, in 2020. He is currently working towards the Ph.D. degree in the School of Cyber Science and Engineering, Wuhan University, China. His research interests include mobile computing and wireless sensing.



**Ruiying Du** received the B.S., M.S., and Ph.D. degrees in computer science in 1987, 1994, and 2008, from Wuhan University, Wuhan, China. She is a professor at School of Cyber Science and Engineering, Wuhan University. Her research interests include network security, wireless network, cloud computing and mobile computing. She has published more than 80 research papers in many international journals and conferences, such as the TPDS, USENIX Security, CCS, INFOCOM, SECON, TrustCom, NSS.



**Yebo Feng** is a research fellow in the School of Computer Science and Engineering (SCSE) at Nanyang Technological University (NTU). He received his Ph.D. degree in Computer Science from the University of Oregon (UO) in 2023. His research interests include network security, blockchain security, and anomaly detection. He is the recipient of the Best Paper Award of 2019 IEEE CNS, Gurdeep Pall Graduate Student Fellowship of UO, and Ripple Research Fellowship. He has served as the reviewer of IEEE TDSC, IEEE TIFS, ACM TKDD, IEEE

JSAC, IEEE COMST, etc. Furthermore, he has been a member of the program committees for international conferences including SDM, CIKM, and CYBER, and has also served on the Artifact Evaluation (AE) committees for USENIX OSDI and USENIX ATC.



**Qingchuan Zhao** is an assistant professor in the Department of Computer Science at the City University of Hong Kong. Prior to joining the department in 2021, he completed his Ph.D. at Ohio State University in the same year, following his M.S. degree from the University of Florida in 2015, and a B.E. degree from South China University of Technology in 2009. His research focuses on the security and privacy practices in the Android appified ecosystem. He employs both static and dynamic data flow analysis on mobile apps and delves into hardware

side channels to uncover a variety of vulnerabilities, including privacy leakage, privilege escalation, and vulnerable access controls. His work has been granted bug bounties from industry-leading companies and has garnered significant media attention.



**Cong Wu** is currently a Research Fellow at Cyber Security Lab, Nanyang Technological University, Singapore. He received Ph.D. degree at School of Cyber Science and Engineering, Wuhan University in 2022. His research interests include AI system security and Web3 security. His leading research outcomes have appeared in USENIX Security, ACM CCS, IEEE TDSC, TMC.